

## RESEARCH PAPER

## Antifungal effect of solid lipid nanoparticles loaded with atorvastatin against *Candida* yeast species as the most common cause of denture stomatitis

Tahereh Molania<sup>1</sup>, Majid Saeedi<sup>2</sup>, Sayed Mohammad Hassan Hashemi<sup>3</sup>, Melika Mollaei<sup>4</sup>, Shidrokh Abootorabi<sup>5</sup>, Maedeh Salehi<sup>1</sup>, Amirhossein Moaddabi<sup>6</sup>, Atefeh Ramzani<sup>7</sup>, Leila Faeli<sup>8,9</sup>, Fatemeh Godarzi Moghadam<sup>10</sup>, Maryam Moazeni<sup>8,9\*</sup>

<sup>1</sup>Department of Oral Medicine, Dental Research Center, Faculty of Dentistry, Mazandaran University of Medical Sciences, Sari, Iran

<sup>2</sup>Pharmaceutical Sciences Research Center, Haemoglobinopathy Institute, Mazandaran University of Medical Sciences, Sari, Iran

<sup>3</sup>Department of Pharmaceutics, Faculty of Pharmacy, Hormozgan University of Medical Sciences, Bandar Abbas, Iran

<sup>4</sup>Dental Research Center, Student Research Committee, Faculty of Dentistry, Mazandaran University of Medical Sciences, Sari, Iran

<sup>5</sup>Department of Pharmaceutics, Faculty of Pharmacy, Hormozgan University of Medical Sciences, Bandar Abbas, Iran

<sup>6</sup>Department of Oral and Maxillofacial Surgery, Dental Research Center, Faculty of Dentistry, Mazandaran University of Medical Sciences, Sari, Iran

<sup>7</sup>Department of Prosthodontics, Dental Research Center, Faculty of Dentistry, Mazandaran University of Medical Sciences, Sari, Iran

<sup>8</sup>Invasive Fungi Research Center, Communicable Diseases Institute, Mazandaran University of Medical Sciences, Sari, Iran

<sup>9</sup>Department of Medical Mycology, School of Medicine, Mazandaran University of Medical Sciences, Sari, Iran

<sup>10</sup>Department of Periodontology, Faculty of Dentistry, Tehran University of Medical Sciences, Tehran, Iran

### ABSTRACT

**Objective(s):** Statins have been used to treat denture stomatitis due to their antifungal properties. However, the side effects associated with these drugs have limited their broader application. This study aimed to evaluate the antifungal effects of solid lipid nanoparticles (SLNs) loaded with atorvastatin (AT-SLN) against the most common *Candida* species, *Candida albicans* and *Candida glabrata*, which are frequently implicated in denture stomatitis.

**Materials and Methods:** AT-SLN was synthesized using an ultrasonication method in this experimental study. The minimum inhibitory concentrations (MICs) of 11 *C. albicans* and 5 *C. glabrata* isolates were determined against AT-SLN, atorvastatin (AT), and nystatin (NYS), following the Clinical & Laboratory Standards Institute (CLSI) guidelines (M27-A3 and M27-S4).

**Results:** The results showed that AT-SLN exhibited the lowest polydispersity index with the optimal hydrophilic-lipophilic balance. Significant differences were observed in the MICs of AT-SLN, AT, and NYS against both *C. albicans* ( $P < 0.001$ ) and *C. glabrata* ( $P = 0.005$ ) isolates. AT-SLN-treated isolates demonstrated significantly reduced MICs ( $P < 0.001$ ). No significant differences were found in the inhibitory effects of AT ( $P = 0.542$ ) and NYS ( $P = 0.526$ ) between *C. albicans* and *C. glabrata*.

**Conclusion:** The findings suggest that AT-SLN may represent a promising antifungal agent for treating denture stomatitis. Further in vivo studies are warranted to confirm these results.

**Keywords:** Atorvastatin, *Candida*, nanoparticles, Antifungal effect

### How to cite this article

Conceição RA; Silva JVV; Prado LD; Patricio BFC. The use of nanocarriers for drug delivery through the blood-brain barrier. *Nanomed J.* 2025; 12: 1-. DOI: 10.22038/NMJ.2025.79926.1974

### INTRODUCTION

**Denture stomatitis** refers to a chronic infection of the mucosal membrane in the oral cavity, commonly observed in individuals who wear dentures [1]. Epidemiological studies indicate that denture stomatitis affects 15 to 70% of denture users [2]. *Candida* species are the primary

pathogens responsible for denture stomatitis, due to their high affinity for binding to the acrylic resin components of dentures [3]. In such cases, antifungal treatment over 12–14 days can be effective [2]. Miconazole, an antifungal agent available in gel form, is used to treat denture stomatitis, but it can cause severe bleeding in patients on anticoagulant therapy [4]. Nystatin (NYS), the gold standard for treating denture stomatitis, is available in various forms, including liquid suspension, cream, and pastilles. However, it

\*Corresponding author(s) Email: moazeni.maryam@gmail.com  
Note. This manuscript was submitted on May 15, 2024; approved on August 14, 2024

has been associated with side effects such as allergic reactions, burning sensations, and gastrointestinal discomfort [5].

**Statins** are widely used to lower serum cholesterol levels and treat cardiovascular diseases. These medications work by inhibiting the synthesis of hydroxymethylglutaryl coenzyme-A reductase, an enzyme critical in the production of cholesterol [6]. Fungi utilize the same metabolic pathway for this enzyme, but instead of cholesterol, their end product is ergosterol. As a result, statins demonstrate significant inhibitory effects on fungal activity. Moreover, statins can disrupt isoprenoid synthesis, leading to lipid alterations and mitochondrial abnormalities in the plasma membrane of *Candida albicans* (*C. albicans*) [7]. Atorvastatin, a third-generation statin, is more effective against fungi than conventional treatments such as nystatin (NYS) and fluconazole [8]. However, statin use can be associated with adverse effects, including statin-associated muscle symptoms, neurocognitive disorders, renal toxicity, hepatotoxicity, and gastrointestinal problems [9]. A growing emphasis is on developing formulations with enhanced effectiveness and improved absorption at lower doses to reduce statin intolerance. In terms of efficacy and biosafety, nanotechnology-based formulations may provide a therapeutic advantage over traditional formulations [10].

**Furthermore**, in conventional drug delivery systems, the distribution of the drug significantly impacts its availability. The therapeutic efficacy of medications in such systems can vary, as the drug concentration may fluctuate before reaching the target tissue. This can result in acute toxicity or reduced effectiveness [11]. Nanotechnology has simplified the delivery of drugs with complex structures. The unique properties of nanoparticles, including their small size, high surface-to-volume ratio, stability, specificity, reduced toxicity, biocompatibility, enhanced patient compliance, and lower treatment costs, offer significant advantages [12, 13]. Additionally, nanotechnology enhances the performance of statins by improving cellular endocytosis, bioabsorption, and overall drug efficacy [14]. Solid lipid nanoparticles (SLNs), a class of nanocarriers, have gained considerable attention in recent years. SLNs offer numerous advantages over conventional drug formulations, including excellent physical stability, high tolerability, and ease of production and scaling [15]. Due to their ability to significantly increase the penetration of drugs into the skin and their lack of notable interactions with the stratum corneum or other skin layers, SLNs are considered an ideal

platform for efficient drug delivery through the skin [16]. SLNs consist of uniformly distributed lipids in an aqueous surfactant solution [17].

Given the challenges posed by *Candida* species and the need for a safe therapeutic approach to minimize the side effects associated with this opportunistic pathogen, the present study aims to investigate the laboratory effects of atorvastatin on the most common *Candida* species: *C. albicans* and *C. glabrata* (recently reclassified as *Nakaseomyces glabratus*).

## MATERIALS AND METHODS

### **Atorvastatin Calcium-Solid Lipid Nanoparticle (AT-SLN) Production**

The ultrasonication method was used to prepare Atorvastatin Calcium-Solid Lipid Nanoparticles (AT-SLNs) [18]. Atorvastatin (AT) tablets (Hakim Pharmaceuticals, Tehran, Iran) were combined with molten glyceryl monostearate (GMS) (Merck, Darmstadt, Germany) using a heating stirrer, with the temperature of GMS maintained below 80°C. Tween 80 and Span 80 (Merck, Darmstadt, Germany) were dissolved in water and heated to 80°C using an 11,000 rpm silent crusher M (Heidolph, Schwabach, Germany). To create a pre-emulsion, the surfactant solution was mixed dropwise with the lipid component under stirring. The resulting pre-emulsion was sonicated (amplitude 20%) with a probe sonicator (Bandelin Sonoplus HD 3100, Berlin, Germany) for 10 minutes to form a nano-emulsion. After sonication, an ice bath was used immediately to convert the nano-emulsion into a nanosuspension [19-21].

### **Assessment of particle size, the polydispersity index, and zeta potential**

The polydispersity index (PDI) and size of the SLN preparations were assessed at 25°C using dynamic light scattering (DLS) with a Mastersizer 200 (Malvern Panalytical Technologies, Malvern, UK), coupled with a Zetasizer Nano ZS system (Malvern Instruments, Worcestershire, UK). The zeta potential of the SLNs was evaluated using laser Doppler electrophoresis [22, 23].

The concentration of atorvastatin (AT) encapsulated in the SLNs was determined using a centrifugation technique. The SLN nanoparticles were centrifuged at 4°C for two hours at 27,000 rpm using a SIGMA 3-30KS refrigerated centrifuge (Osterode am Harz, Germany). The resulting supernatant was filtered, diluted by a factor of 100, and analyzed for AT content (unbound drug) using high-performance liquid chromatography (HPLC) (Knauer, Berlin, Germany). The HPLC mobile phase consisted of a 30:70 (v/v) mixture of water (pH 3,

adjusted with 80% phosphoric acid) and methanol [24]. The analysis was performed at a 1.0 mL/min flow rate, using an XDB-C18 column with UV detection at 238 nm. All assessments were conducted at 25°C, with an injection volume of 20 µL and a runtime of approximately 30 minutes. To determine the drug encapsulation efficiency (EE%), Equation 1 was used.

$$EE\% = \frac{(W_{\text{initial}} - W_{\text{free}})}{W_{\text{initial}}} \times 100 \quad [18]$$

The morphology of the niosomes was examined using scanning electron microscopy (SEM). Gold coating was applied to create the DSR1 nanostructure using a desk sputter coater. The SEM (Hitachi S-4160, Ibaraki, Japan) was operated at an acceleration voltage of 20.0 kV and magnification of 15,000x.

Atomic Force Microscopy (AFM, JPK Instruments) was used to study the morphology of the nanoparticles. The nanoparticles were diluted 500 times and dried at room temperature before being applied to the sample stage. Repulsive forces were used to capture images in contact mode.

Microscopic analysis was also conducted using transmission electron microscopy (TEM) (Hitachi H-7500, Ibaraki, Japan) at a voltage of 120 kV. The SLN samples were diluted 1:2 with purified water before use. The diluted samples were placed on a 200-mesh carbon-coated copper grid, stained with 2% phosphotungstic acid, and then dried [25].

Differential scanning calorimetry (DSC) was performed using a Pyris 6 DSC system (PerkinElmer, Waltham, MA, USA) to obtain thermograms of the specimens (drug, lipid, and AT-SLN in lyophilized form). Approximately 5 mg of each specimen was used for each analysis, and all samples were placed in sealed aluminum pans. The pans containing the ingredients or formulations were heated at a rate of 10 °C/min from 30 to 300 °C. Indium was used for DSC calibration [26].

The AT-SLN was lyophilized at -80 °C and 0.1 mbar (Marin Christ, Osterode, Germany) for 48 hours. Attenuated total reflectance Fourier transform infrared (ATR-FTIR) spectroscopy was performed on AT, GMS, Tween 80, Span 80, and AT-SLN powder. For each analysis, 5 mg of each uniform specimen was placed on the ATR window, and the spectra were recorded in the wavenumber range of 4000–400 cm<sup>-1</sup> with a resolution of 2 cm<sup>-1</sup> [27].

#### **In vitro drug release**

In the in vitro drug release assessment, acetate cellulose membranes with a molecular weight cutoff of 12 kDa and in vitro release immersion cells were used [28]. The acetate cellulose membrane

was applied after sealing the cells with caps and placing the samples inside. The cells were then placed in the USP dissolution apparatus No. 2, which contained 900 mL of an ethanol-water mixture in equal proportions. At specified intervals, 5 mL of the dissolution medium was withdrawn, filtered through a 0.22 µm filter, and analyzed by HPLC. After each sampling, 5 mL of the ethanol-water mixture was replenished to maintain a constant volume of dissolution medium.

#### **In vitro cell viability study**

The human foreskin fibroblast (HFF) cells used in the in vitro cytotoxicity analysis of AT, blank SLN, and AT-SLN formulations were obtained from the National Cell Bank, Pasteur Institute of Iran, Tehran, Iran. The cells were seeded at a density of 10<sup>5</sup> cells/well in the bottom of 96-well microplates and incubated for 24 hours. The wells were then treated with blank SLN, AT-SLN, or AT (at concentrations of 0.5, 1, 1.5, 2, and 2.5 µM). After treatment, the cells were washed with phosphate-buffered saline (PBS). Cell viability was assessed using the MTT colorimetric assay. MTT (0.5 mg/mL) was added, and the cells were incubated for 4 hours at 37 °C. After removing the supernatant, the formazan crystals were dissolved in 100 µL of dimethyl sulfoxide (DMSO). Following agitation of the plates for 20 minutes, the optical density was measured at 560 nm using a multi-well spectrophotometer. The cell viability was determined by performing three independent tests in duplicate, with six control wells (cells in media) at each concentration. The viability was calculated using the following formula:

$$\text{Viability (\%)} = \left[ \frac{(\text{OD}_{\text{sample}} - \text{OD}_{\text{blank}})}{\text{OD}_{\text{control}} - \text{OD}_{\text{blank}}} \right] \times 100 \quad [24]$$

Where OD control and OD sample denote the optical density (control) and the optical density (sample) at 560 nm, respectively.

#### **Antifungal agents**

Atorvastatin, AT-SLNs, and NYS were evaluated for antifungal susceptibility testing (AFST). NYS was dissolved in dimethyl sulfoxide (DMSO), diluted two-fold, and added to RPMI 1640 medium containing L-glutamine without bicarbonate. The pH of the medium was then adjusted to 7.0 using a 0.165 M solution of 3-N-morpholinopropanesulfonic acid (Sigma Chemical Co., St. Louis, MO, USA), a highly effective buffer for maintaining nearly neutral pH in various biological systems. Two-fold serial dilutions of each agent were also prepared (29).

### Antifungal susceptibility assay

Minimum inhibitory concentrations (MICs) against atorvastatin, AT-SLNs, and NYS were determined for 11 isolates of *C. albicans* and five isolates of *C. glabrata*, following the Clinical and Laboratory Standards Institute (CLSI) M27-A3 and M27-S4 guidelines [29]. In 96-well microdilution trays, AT (1–32 µg/mL) and AT-SLNs (0.015–0.5 µg/mL) were dispensed at final concentrations. These concentrations were selected based on the results of pilot studies. Additionally, for each strain, one well was dedicated to blank SLNs (without AT) to assess the potential effect of the SLN composition on yeast growth. ITS sequencing previously identified the isolates as *C. albicans* and *C. glabrata*. Yeast suspensions were prepared by mixing fresh yeast colonies with 5 mL of distilled water. The optical density of the suspensions was adjusted to 0.09–0.13, corresponding to a transmission of 75–77% at 530 nm. The suspension was then diluted in RPMI medium, first 1:10 and then 1:100, to achieve the final inoculum, which resulted in a concentration of approximately  $1 \times 10^3$  to  $5 \times 10^3$  CFU/mL. The plates were incubated at 35°C for 24 hours, after which the drug concentration that completely inhibited growth compared to the control was recorded. Due to the self-turbidity of AT-SLNs, the results were examined using an inverted microscope (Motic AE31, Hong Kong, China). Quality control strains, *C. krusei* (ATCC 6258) and *C. parapsilosis* (ATCC 22019), were used to assess the accuracy of the antifungal susceptibility testing (AFST) assay. The MIC results for the strains against the antifungal agents were determined and reported according to the CLSI guidelines.

### Statistical analysis

Data analysis was performed using descriptive and inferential statistics in SPSS software (version 26, SPSS Inc., Chicago, IL, USA). Frequent

distributions, percentages, means, and standard deviations were calculated for descriptive statistics. In the inferential statistics section, analysis of variance (ANOVA), Bonferroni adjustment, independent t-tests, and paired t-tests were employed. Chi-square and Fisher's exact tests were used for nominal variables. To assess reproducibility, each test was repeated twice on different days and performed in duplicate.

## RESULTS

### Evaluation of AT-SLN characteristics

Ultrasonication was used to generate SLNs containing AT. The hydrophilic-lipophilic balance (HLB) values were assessed by employing different ratios of the binary mixture of Tween 80 and Span 80 to optimize the formulation of AT-SLNs. The nanoparticle diameter was a key factor in this study, and special attention was given to this parameter. Table 1 shows the hydrodynamic size of the SLNs (z-average diameter/intensity-weighted average diameter) and the polydispersity index (PDI), which indicates the dispersion of particle sizes. The PDI typically ranges from 0 to 1, with values higher than 0.70 indicating a sample containing a wide range of particle sizes [30]. The PDI ranged from  $0.485 \pm 0.036$  to  $0.437 \pm 0.013$ . Notably, the SLN with the highest HLB (F4) exhibited the lowest PDI value ( $0.437 \pm 0.013$ ). The results also showed that the zeta potential of the different preparations ranged from  $-20.46 \pm 0.47$  mV (F4) to  $-27.1 \pm 0.3$  mV (F1). Furthermore, the various preparations' encapsulation efficiency (EE%) varied from  $46.44 \pm 0.47\%$  to  $85.88 \pm 0.30\%$ . The morphology and shape of the nanoparticles were assessed using scanning electron microscopy (SEM), transmission electron microscopy (TEM), and atomic force microscopy (AFM). SEM, TEM, and AFM images of F1 (Figure 1) revealed that the particles were spherical, uniform, and well-separated in the AFM image.

Table 1. Formulations for AT-SLN and physicochemical data (mean  $\pm$  SD).

Formulation	AT (mg)	GMS (mg)	Span 80 (mg)	Tween 80 (mg)	Water up to 50 ml	HLB	Particle size (nm)	PDI	Zeta potential (mv)	EE (%)
F1	500	1000	740	860	50	10	236.20 $\pm$ 6.13	0.485 $\pm$ 0.036	-27.1 $\pm$ 0.3	85.88 $\pm$ 0.30
F2	500	1000	450	1150	50	12	229.26 $\pm$ 2.44	0.481 $\pm$ 0.017	-23.43 $\pm$ 0.05	69.44 $\pm$ 0.28
F3	500	1000	150	1450	50	14	213.53 $\pm$ 8.29	0.458 $\pm$ 0.033	-21.66 $\pm$ 1.04	51.65 $\pm$ 1.04
F4	500	1000	0	1600	50	15	188.93 $\pm$ 7.44	0.437 $\pm$ 0.013	-20.46 $\pm$ 0.47	46.44 $\pm$ 0.47

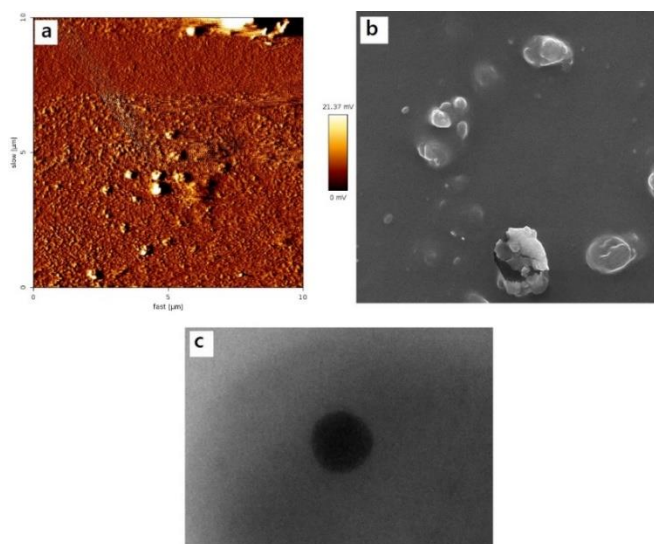


Fig. 1. (a) AFM, (b) SEM and (c) TEM image of F1

ATR-FTIR spectroscopy assessed the chemical interactions between the drug and the ingredients in the SLN formulation. The ATR-FTIR spectra of AT, GMS, Tween 80, Span 80, and F1 are shown in Figure 2. The ATR-FTIR analysis of AT displayed characteristic bands at specific wavenumbers, including 3668  $\text{cm}^{-1}$  and 3249  $\text{cm}^{-1}$  for O–H stretching, 2972  $\text{cm}^{-1}$  for N–H stretching, 1649  $\text{cm}^{-1}$  for C=O (amide) stretching, 1435  $\text{cm}^{-1}$  for C–F stretching, 1317  $\text{cm}^{-1}$  for C–O stretching, 1215  $\text{cm}^{-1}$  for C–N stretching, and 690  $\text{cm}^{-1}$  for aromatic out-of-plane bending. The major bands in the GMS ATR-FTIR spectra were observed at 3400–3200  $\text{cm}^{-1}$  (O–H stretching), 3000–2850  $\text{cm}^{-1}$  (C–H stretching), 1730  $\text{cm}^{-1}$  (C=O stretching), and 1300–1000  $\text{cm}^{-1}$

(C–O stretching). The ATR-FTIR spectra of Tween 80 revealed prominent peaks at 3497  $\text{cm}^{-1}$  (O–H stretching), 2922  $\text{cm}^{-1}$  (–CH<sub>2</sub>–CH<sub>2</sub>–asymmetric stretching), 2858  $\text{cm}^{-1}$  (–CH<sub>2</sub>–symmetric stretching), and 1735  $\text{cm}^{-1}$  (C=O stretching). The spectra of Span 80 showed distinctive peaks at 3400  $\text{cm}^{-1}$  (O–H stretching), 2923  $\text{cm}^{-1}$  (–CH<sub>2</sub>–CH<sub>2</sub>–asymmetric stretching), 2854  $\text{cm}^{-1}$  (–CH<sub>2</sub>–symmetric stretching), and 1739  $\text{cm}^{-1}$  (C=O stretching). The ATR-FTIR analysis of formulation F1 showed no evidence of chemical interaction between the drug and ingredients, as the principal diagnostic peaks for AT were still visible in the F1 formulation's ATR-FTIR spectrum.

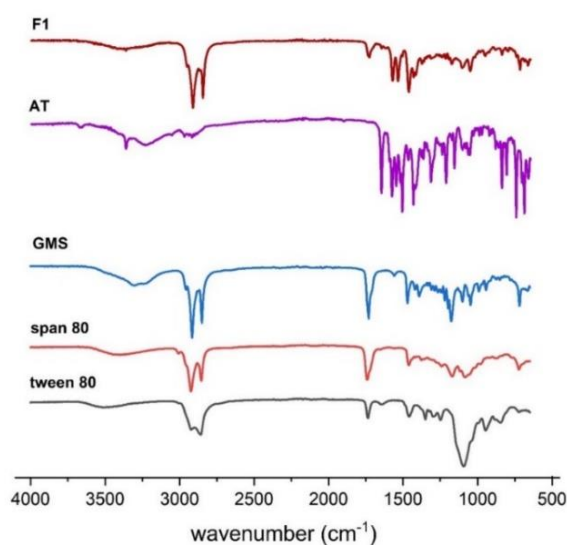


Fig. 2. ATR-FTIR AT-SLN (F1), AT, GMS, span 80 and tween 80

Figure 3 displays the DSC results for GMS, AT, and the optimal formulation powder (F1). In the DSC analysis, GMS exhibited a sharp endothermic peak at 64.53°C, corresponding to its melting point. The DSC trace of AT showed three distinct phases at the following temperatures: 80.87 to 137.17°C, 137.17 to 176.85°C, and 195.19 to 289.24°C. These phases are associated with water loss, the melting point,

and the decomposition of AT (phase transition). The results of the in vitro AT-SLN release experiment are shown in Figure 4. Adding AT to SLN formulations increased the drug dissolution rate, as evidenced by comparing the SLN formulation with the control. The percentage of AT released from F1 and the power were 80% and 47%, respectively.

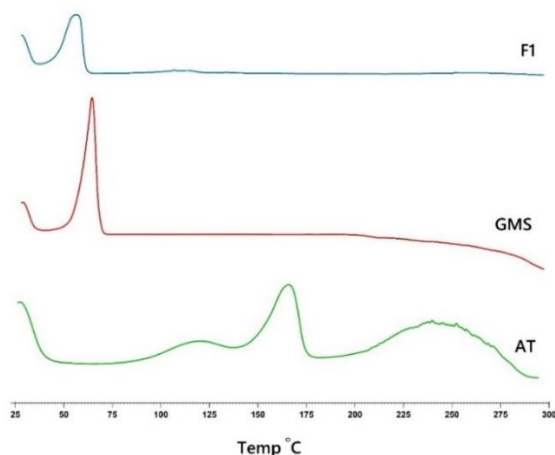


Fig. 3. DSC thermogram of AT-SLN (F1), GMS and AT

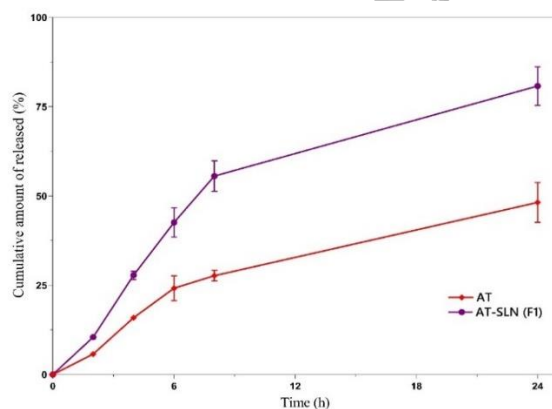


Fig. 4. In vitro drug release of AT and AT-SLN (F1)

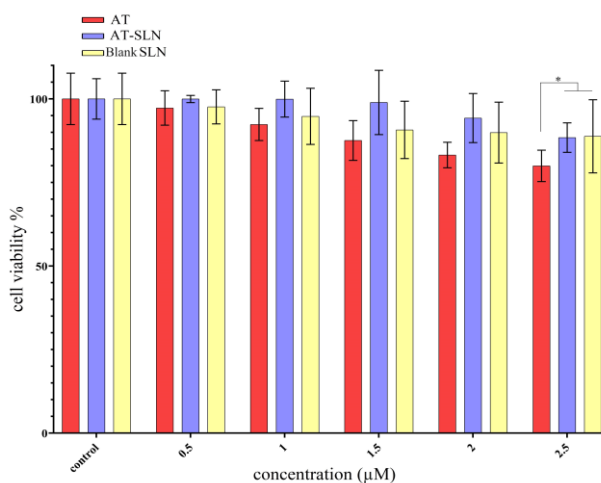


Fig. 5. In Vitro Cell Viability Study of AT, blank SLN and AT-SLN (F1)

**In vitro cell viability study**

The MTT assay is used to assess the metabolic activity of living cells and relies on absorbance measurements. The human foreskin fibroblast (HFF) cell line was cultured with varying concentrations of blank SLN, free AT, and AT-SLN (0.5–2.5 µM) for 24 hours to evaluate the effects of AT-SLN on cell viability (Figure 5). When blank SLN and AT-SLN were used at comparable concentrations (0.5–2.5 µM), no significant decrease in cell viability was observed over 24 hours ( $P > 0.05$ ). The results indicated that after 24 hours of treatment with blank SLN and AT-SLN (2.5 µM), 91.79% and 92.41% of the cells remained viable, respectively. In contrast, AT treatment resulted in only 79.9% cell viability. These findings suggest that AT was cytotoxic to the HFF cell line, while AT-SLN showed no cytotoxicity. This is consistent with the findings of Çelik et al., who demonstrated that different AT concentrations increased the cytotoxicity in human neuroblastoma cell lines (SH-SY5Y) [31]. Furthermore, Abootorabi et al. reported that encapsulating AT in niosomes can enhance the viability of HFF cells [24]. The results were validated by checking reproducibility,

with the tests repeated twice on different days and conducted in duplicate.

**Antifungal susceptibility tests**

The antifungal effects of NYS, AT, and AT-SLNs on *C. albicans* and *C. glabrata* are summarized in Table 2. For the 16 strains studied, no significant differences were observed in the MIC<sub>50</sub> concentrations between NYS and AT ( $P > 0.05$ ). However, when comparing the NYS and AT groups, significant differences were noted in the MIC ranges when the strains were exposed to AT-SLNs. In the case of *C. glabrata*, no significant decrease in MICs was observed between the NYS and AT-SLN groups. Despite this, the differences between AT and AT-SLNs remained significant, indicating that the SLN formulation affected the antimicrobial activity of AT (Table 3 and Figure 6). Furthermore, when exposed to blank SLNs, the yeast strains exhibited growth similar to the positive control (without any drug treatment), indicating that the SLN composition did not show antifungal activity. The results were validated by checking reproducibility, with the tests repeated twice on different days and conducted in duplicate.

**Table 2.** Comparison between MICs values of AT-SLN, AT, and NYS achieved for *C. albicans* and *C. glabrata*.

Candida species	Drugs	MICs (µg/ml)												MICs parameters (µg/ml)		
		0.015	0.031	0.0625	0.125	0.25	0.5	1	2	4	8	16	32	Range	MIC <sub>50</sub> / MIC <sub>90</sub> *	GM**
<i>C. albicans</i> (n=11)	NYS								7	4				2-4	2/4	2.57 3
	AT							2	5		2	1	1	1-32	2/16	3.52 6
	AT-SLN	4	2	1		3	1							0.015 -0.5	0.031 / 0.25	0.05 8
<i>C. glabrata</i> (n=5)	NYS							4	1					1-2	-	1.14 9
	AT							1	3		1			1-8	-	2.29 7
	AT-SLN					4	1							0.25- 0.5	-	0.28 7
All <i>Candida</i> species (n=16)	NYS							4	8	4				1-4	2/4	2
	AT							3	8		3	1	1	1-32	2/8	3.08 4
	AT-SLN	4	2	1		7	2							0.015 -0.5	0.25/ 0.25	0.09 5

\*MIC<sub>50</sub> concentration (50% of inhibited isolates), and MIC<sub>90</sub> (90% of inhibited isolates).

\*\*GM, geometric mean

**Table 3.** Comparison between MIC values achieved for AT-SLN, AT, and NYS

<i>Candida</i> species	groups	Mean ± Standard deviation (SD)	Coefficient of variation	P value (AT-SLNs and NYS)
<i>C. albicans</i>	AT-SLN	0.130 ± 0.160	132	P < 0.001
	AT	6.90 ± 9.51	137	
	NYS	2.72 ± 1.009	37	
<i>C. glabrata</i>	AT-SLN	0.300 ± 0.111	37	P= 0.005
	AT	3 ± 282	94	
	NYS	2.40 ± 0.89	37	

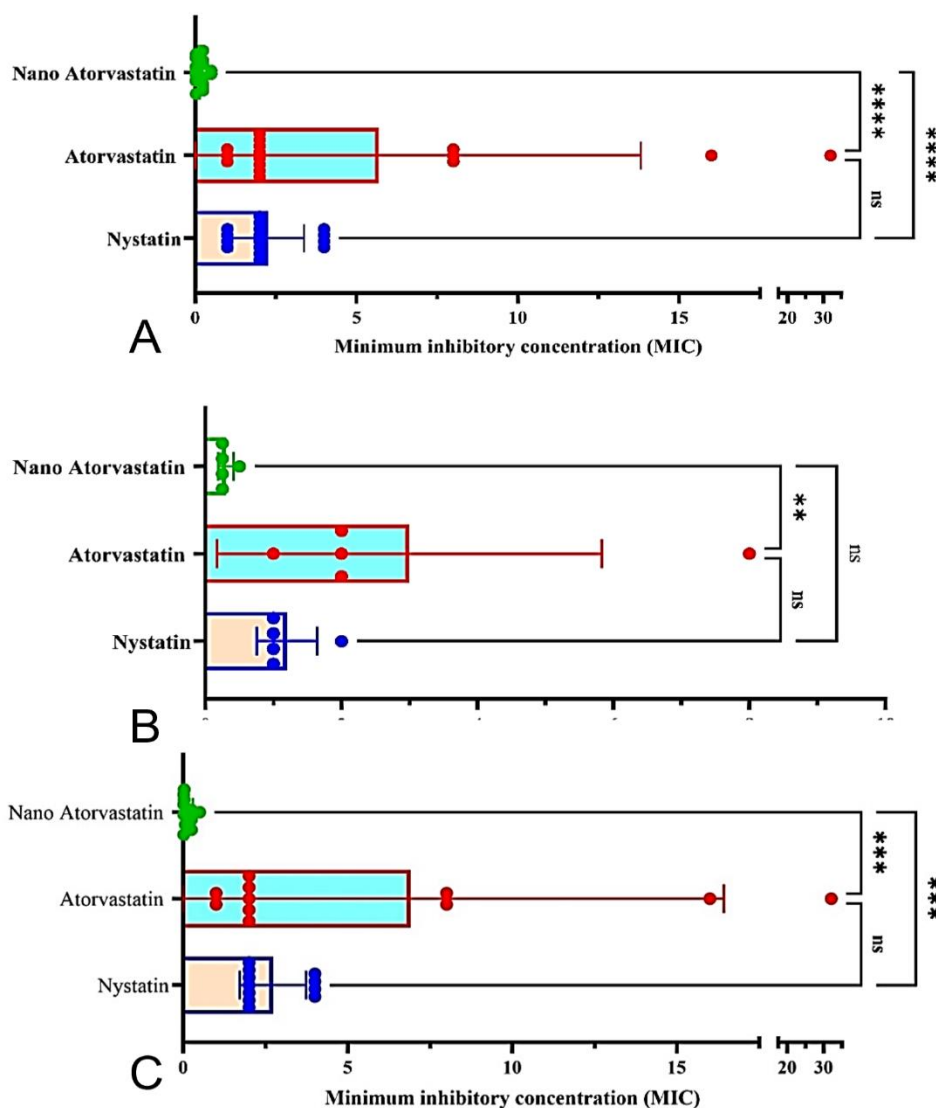


**Fig. 6.** Effect of the AT-SLN, AT and NYS on strains of *C. albicans* (A), *C. glabrata* (B), and significant antifungal effect of AT-SLNs compare with NYS in all strains of *Candida* species, generally.

## DISCUSSION

Atorvastatin is rapidly absorbed when administered orally, reaching its peak concentration within one to two hours; however, it has low bioavailability. To enhance the drug's effectiveness, new methods are recommended to address absorption and dissolution challenges [32]. The present study evaluated the in vitro activity of

NYS, AT, and AT-SLN against the growth of *C. albicans* and *C. glabrata*.

Based on our findings, a decrease in the HLB value of binary surfactant combinations from 15 (F4) to 10 (F1) resulted in an increase in the AT-SLN particle diameter from  $188.93 \pm 7.44$  nm to  $236.20 \pm 6.13$  nm ( $P = 0.05$ ). Span 80, a low HLB surfactant, should be used in larger amounts to create a

formulation with a lower HLB value; as a result, Span 80 aids in incorporating more drug into the SLN. Larger emulsion droplets are expected when the HLB value is optimized during production. Additionally, using binary surfactant combinations can enhance the stability of the formulation. Better emulsion droplet stability is achieved by using binary combinations of surfactants with high and low HLB values, as these surfactants are distributed in the oil and aqueous phases, respectively [33]. The surfactant with the lowest HLB value tends to be distributed in the oil phase, forming a stable film at the interface of the phases [34]. Hahraeini et al. (2020) reported that decreasing the HLB (Tween 40 and Span 80) from 15.6 to 9.1 increased the naproxen-SLN diameter from 71.07 to 202.07 nm [35]. Additionally, Rostamkalaei et al. (2019) found that decreasing the HLB value from 11.67 to 8.45 increased the diameter of metformin-loaded SLNs from 203 to 389 nm [36]. Finally, Saeedi et al. (2019) demonstrated that the diameter of venlafaxine-SLNs increased from  $77.00 \pm 4.35$  to  $311.33 \pm 9.29$  nm due to a decrease in HLB from 15 to 8 [20].

The SLN dispersions produced with a binary surfactant combination had a PDI value 0.4, indicating a satisfactory SLN size distribution. According to Shahraeini et al., there was a slight variation in the PDI of atorvastatin SLNs when the HLB value was increased in the formulation; however, this variation was not significant ( $P > 0.05$ ) [35]. Nanoparticles typically have a PDI between 0 and 1. Values greater than 0.7 suggest a broad distribution of sizes, while a PDI of less than 0.3 indicates a highly homogeneous population. The generated SLNs had a PDI value of  $\leq 0.5$ , which is considered suitable based on the criteria outlined in Table 1 [37, 38].

The findings showed that the zeta potential for these solutions (containing non-ionic surfactants) ranged from  $-20.46 \pm 0.47$  mV (F4) to  $-27.10 \pm 0.3$  mV (F1) ( $P < 0.001$ ). This negative charge surrounding the particles could be attributed to residual electrolyte from the ethoxylation catalyst of the non-ionic surfactants [39] or the dipole character of the ethoxy groups in Tween and Span [40]. As shown in Table 1, increasing the amount of Span 80 in the formulation led to a rise in the zeta potential. A stable surfactant film is generally expected to form at the interface of emulsion droplets when a binary combination of surfactants is at its optimal level, resulting in finer droplets with increased stability [41]. An increase in Span concentration appears to create a more compact barrier around the particles, thereby enhancing their negative charge (Table 1). Overall, the zeta potential value reflects the Stern layer (the

presence of free drug in the aqueous medium) and the particle surface charge (the presence of lipids and surfactants).

A decrease in the HLB value leads to an increase in the size, EE%, and zeta potential (indicating greater stability) of the nanoparticles, as shown in Table 1. Since the drug's solubility and miscibility in the lipid matrix can affect loading amounts, atorvastatin's high solubility in Span 80 (the calcium form of atorvastatin is soluble in Span 80 at 47.47 mg/mL) may explain the increased EE%, which results from a decrease in the HLB value [42]. A reduction in the HLB value is correlated with an increase in Span 80 concentration, which may enhance the loading of atorvastatin ( $\log P = 6.98$  and water solubility of 0.00063 mg/mL) into the solid lipid. Additionally, studies have shown that as particle diameter decreases, the specific surface area increases proportionally, while drug loading and EE% decrease (31, 34). Other investigations by the authors have demonstrated that higher solubility of naproxen in Span 80 ( $\log P = 3.39$  and water solubility of 0.0299 mg/mL) or increased particle size in metformin ( $\log P = -1.8$  and water solubility of 1.38 mg/mL) could contribute to a higher percentage of EE% [36].

The new approach for manufacturing AT-SLN offers an advantage over previous techniques due to the absence of organic solvents. Additionally, no studies have yet explored the effect of the Span: Tween ratio on the efficiency of AT encapsulation in SLNs. The nanoparticles in this study were designed to possess the ideal characteristics, including appropriate size, narrow size distribution, high zeta potential, and enhanced EE%. Achieving nanoparticles that meet all of these criteria is challenging. Consequently, F1 was selected for further research due to its optimal particle size ( $236.20 \pm 6.13$  nm), high drug encapsulation efficiency ( $85.88 \pm 0.30\%$ ), and the highest zeta potential ( $-27.1 \pm 0.3$  mV), with a PDI of  $0.485 \pm 0.036$ .

When comparing the DSC profiles of GMS and atorvastatin with AT-SLN, only one endothermic peak is observed near the GMS melting point, and no endothermic peak corresponding to atorvastatin melting is detected. This suggests that atorvastatin in the SLN preparations may be present in a molecular or crystalline form that is not identifiable due to the minimal amount of atorvastatin in the formulation. Additionally, the characteristic peak of atorvastatin may be absent if it dissolves in molten GMS. The formulation also shows endothermic peaks at slightly lower temperatures. For example, the GMS endothermic peak appears at  $54.46^\circ\text{C}$ , instead of its expected value of  $64.53^\circ\text{C}$ . These

variations and the decrease in the melting point could be attributed to the particles' large specific surface area and nanometric diameter (large surface-to-volume ratio) [43].

The presence of surfactants (Span 80 and Tween 80) in solid lipid nanoparticle (SLN) formulations may cause a shift in the GMS melting peak. This finding is consistent with the research by Trivino et al. [44], who used differential scanning calorimetry (DSC) to evaluate the miscibility of drug-lipid-surfactant combinations. Their study suggested that the miscibility of GMS with surfactants could reduce its melting point when combined with these surfactants. Furthermore, another study observed that the decrease in GMS's melting temperature in SLN formulations was due to its transformation into the stable  $\beta$  phase during the heating and cooling cycles of the SLN preparation process, a phenomenon that has been extensively investigated in other studies [45, 46].

Figure 4 confirms no transition or decomposition was observed during the SLN preparation. The authors suggested that the dissolution of AT in the molten lipid/surfactant mixture throughout the DSC run prevents AT molecules from decomposing. No protective effect is observed in the absence of lipid/surfactants in pure AT, which is attributed to the lack of lipid/surfactants. The absence of the AT melting peak in the SLN preparation may be due to the solubility or miscibility of AT in the lipids or surfactants. The thermal behavior of ATR-mannitol or ATR-lactose combined with AT-SLN (containing Tween and Span) yielded similar results in previous studies [18, 47].

As shown in Figure 4, SLNs may enhance poorly soluble drugs' dissolution rate, bioavailability, and drug release. Kelidari et al. observed that spironolactone-loaded SLNs significantly improved the in vitro dissolution rate, potentially facilitating the rapid onset of therapeutic effects [48].

Overuse of antifungal drugs, such as azoles and NYS, has led to the emergence of resistant *Candida* species. However, statins have caused less resistance due to their distinct mode of action [32]. The results in Table 3 show that AT-SLN had the lowest MIC for *C. albicans* (ranging from 0.015 to 0.5 mg/mL). Additionally, the MIC of AT against *C. albicans* and *C. glabrata* was  $6.90 \pm 9.51$  mg/L and  $3.00 \pm 2.82$  mg/L, respectively. The findings of Soares et al. showed that the MIC of AT against *C. albicans* was 25.31  $\mu$ g/mL. While their results were similar to ours regarding AT's antifungal activity, the MIC values reported in the two studies differed (49). In the study by Isfahani et al., the MIC of AT compared to NYS and fluconazole against *C. glabrata* ranged from 2 to 4  $\mu$ g/mL. Their findings

were consistent with ours regarding AT's efficacy against this species [49].

The findings of the present investigation demonstrate that the MIC of AT-SLN against *C. albicans* and *C. glabrata* were  $0.130 \pm 0.160$  mg/L and  $0.300 \pm 0.111$  mg/L, respectively. Since no similar study has been conducted on the effects of the nanoformulation of statins, direct comparison is impossible. However, the results of this study suggest that AT-SLN exhibits greater antifungal activity than the other two compounds mentioned.

Although research on the application of statin drugs using nanotechnology has been conducted, the antifungal effects of these nanocompounds remain underexplored. For example, Morsy et al. reported that AT nano-emulgel showed the highest wound closure percentage and could be a potential new compound for wound healing [50].

According to a study by Lima et al., fluvastatin, rosuvastatin, and atorvastatin (AT) were all highly effective against fungal species, particularly *C. albicans* (MIC < 128–1  $\mu$ g/mL) and *C. glabrata* (MIC 32–64  $\mu$ g/mL). Consistent with the findings of the current study, it was also observed that all statins exhibited greater inhibitory activity against fungi than bacteria [51].

As previously mentioned, the MIC of AT against *C. albicans* and *C. glabrata* was  $6.90 \pm 9.51$  mg/L and  $3.00 \pm 2.82$  mg/L, respectively. Although AT appears more effective against *C. glabrata*, no significant difference was observed in its inhibitory effect between *C. albicans* and *C. glabrata*. In line with our results, Nyilasi et al. reported that the MIC of AT against *C. albicans* and *C. glabrata* was 128 and 32  $\mu$ g/mL, respectively, indicating a more decisive action against *C. glabrata* than *C. albicans* [52].

Bakhtiari et al. investigated the efficacy of cinnamaldehyde and NYS against *C. glabrata* and *C. albicans* and found that the MIC of NYS against *C. albicans* and *C. glabrata* were 0.5 and 4  $\mu$ g/mL, respectively, demonstrating greater efficacy against *C. albicans* [53]. Their findings were consistent with those of the current study; however, no significant difference was observed in the inhibitory effect of NYS ( $P = 0.526$ ) against *C. albicans* and *C. glabrata* in the present investigation.

The present study found that the MIC of *C. albicans* in AT-SLN decreased significantly compared to AT and NYS; however, there was no significant difference in the MIC of *C. albicans* between AT and NYS. In contrast, Esfahani et al. reported statistically significant effects for NYS and AT against *C. albicans* and *C. glabrata*. However, the same study observed no significant difference in

the inhibitory effect of AT on *C. albicans*, *C. glabrata*, or other *Candida* species, which is consistent with our findings [49].

In Brillhante et al.'s investigation, the MIC of simvastatin for *C. albicans* and *Cryptococcus* ranged from 15.6 to 1000 µg/mL and 62 to 1000 µg/mL, respectively. Additionally, simvastatin inhibited the maturation and growth of *C. albicans*. Based on these findings, the authors suggested that simvastatin has a high potential to inhibit the development of planktonic cells, *C. albicans* biofilm, and *Cryptococcus* [54]. In the present study, the MIC of AT against *C. albicans* was  $6.90 \pm 9.51$  µg/mL, and a significant difference was observed between the AT-SLN, AT, and NYS groups in their inhibitory effects on the growth of *C. albicans* in vitro. Thus, both studies confirm the antifungal properties of statins.

The investigation found that nano-statins more effectively inhibited *Candida* than standard AT and azole drugs. Other researchers have also highlighted the superior effectiveness of statin drugs in their nanoform in various fields [55, 56]. Rodrigues et al. obtained similar results by combining two polymers with a nano-system containing simvastatin [57].

Statins have been proven effective against various fungi in laboratory tests; however, their side effects and interactions with azole drugs and immunosuppressants can diminish their benefits [58]. Nanotechnology can enhance drug bioavailability and minimize adverse effects, including for statins [55]. The present study's findings suggest that AT-SLN exhibits effective antifungal properties against both *C. albicans* and *C. glabrata*; however, further studies are needed to evaluate its effectiveness against other *Candida* species. Additionally, studies with larger sample sizes could help validate the current findings.

## CONCLUSION

In conclusion, AT-SLN demonstrated strong antifungal activity against *Candida* species. However, NYS proved to be a more effective agent than AT-SLN against *C. glabrata*. Further studies with more *C. glabrata* strains are recommended to support our findings.

## ACKNOWLEDGEMENTS

The authors would like to thank Mazandaran University of Medical Sciences.

## CONFLICTS OF INTEREST

The authors have declared no competing interests.

## FUNDING

This study was funded by the Mazandaran University of Medical Sciences Research Committee, Sari, Iran (grant number: 4297).

## REFERENCES

1. Ramezani A, Mollaei M, Yazdani Charati J, Tavakolian H, Mesgarani A, Molania T. Prevalence of Denture Stomatitis in Patients Using Denture in Sari City, Iran, in 2020-2021. *Iran J Health Sci.* 2023;11(2):137-142.
2. Gendreau L, Loewy ZG. Epidemiology and etiology of denture stomatitis. *J Prosthodont.* 2011;20(4):251-260.
3. Dadar M, Tiwari R, Karthik K, Chakraborty S, Shahali Y, Dhama K. *Candida albicans*-Biology, molecular characterization, pathogenicity, and advances in diagnosis and control—An update. *Microb Pathog.* 2018;117:128-138.
4. Fakhra DI. Comparison Of The Efficacy And Tolerance Between Miconazole As Chewing Gum And As Gel Application In Patients With Oral Candidiasis. Doctoral dissertation, Bbdcods. 2021.
5. Abuhajar E, Ali K, Zulfiqar G, Al Ansari K, Raja HZ, Bishti S, et al. Management of Chronic Atrophic Candidiasis (Denture Stomatitis)—A Narrative Review. *Int J Environ Res Public Health.* 2023;20(4):3029.
6. Pinal-Fernandez I, Casal-Dominguez M, Mammen AL. Statins: pros and cons. *Med Clin (English Edition).* 2018;150(10):398-402.
7. Sadowska A, Osiński P, Roztocka A, Kaczmarz-Chojnacka K, Zapora E, Sawicka D, et al. Statins—From Fungi to Pharmacy. *Int J Mol Sci.* 2023;25(1):466.
8. Esfahani AN, Golestannejad Z, Khozeimeh F, Dehghan P, Maheronnaghsh M, Zarei Z. Antifungal effect of Atorvastatin against *Candida* species in comparison to Fluconazole and Nystatin. *Med Pharm Rep.* 2019;92(4):368.
9. Ward NC, Watts GF, Eckel RH. Statin toxicity: mechanistic insights and clinical implications. *Circ Res.* 2019;124(2):328-350.
10. Etemad L, Salmasi Z, Kalat SAM, Moshiri M, Zamanian J, Kesharwani P, et al. An overview on nanoplateforms for statins delivery: Perspective study for safe and effective therapy methods. *Environ Res.* 2023;116572.
11. Chenthamara D, Subramaniam S, Ramakrishnan SG, Krishnaswamy S, Essa MM, Lin F-H, et al. Therapeutic efficacy of nanoparticles and routes of administration. *Biomater Res.* 2019;23(1):1-29.
12. Dikmen G, Genç L, Güney G. Advantage and disadvantage in drug delivery systems. *J Mater Eng.* 2011;5(4):468.
13. Moaddabi A, Soltani P, Rengo C, Molaei S, Mousavi SJ, Mehdizadeh M, et al. Comparison of antimicrobial and wound-healing effects of silver nanoparticle and chlorhexidine mouthwashes: An in vivo study in rabbits. *Odontology.* 2022;110(3):577-583.
14. Korani S, Korani M, Bahrami S, Johnston TP, Butler AE, Banach M, et al. Application of nanotechnology to improve the therapeutic benefits of statins. *Drug Discov. Today.* 2019;24(2):567-574.

15. Mehnert W, Mäder K. Solid lipid nanoparticles: production, characterization and applications. *Adv. Drug Deliv Rev.* 2012;64:83-101.
16. Kakadia PG, Conway BR. Solid lipid nanoparticles: a potential approach for dermal drug delivery. *Am J Pharmacol Sci.* 2014;2(5A).
17. Sathali A, Ekambaram P, Priyanka K. Solid lipid nanoparticles: a review. *Sci. Rev. Chem. Commun.* 2012;2(1):80-102.
18. Shahraeini SS, Akbari J, Saeedi M, Morteza-Semnani K, Abootorabi S, Dehghanpoor M, et al. Atorvastatin solid lipid nanoparticles as a promising approach for dermal delivery and an anti-inflammatory agent. *AAPS Pharm Sci Tech.* 2020;21(7):1-10.
19. Boskabadi M, Saeedi M, Akbari J, Morteza-Semnani K, Hashemi SMH, Babaei A. Topical Gel of Vitamin A Solid Lipid Nanoparticles: A Hopeful Promise as a Dermal Delivery System. *Adv Pharm Bull.* 2021;11(4):663.
20. Saeedi M, Morteza-Semnani K, Akbari J, Siahposht-Khachaki A, Firouzi M, Goodarzi A, et al. Brain targeting of venlafaxine HCl as a hydrophilic agent prepared through green lipid nanotechnology. *J Drug Deliv Sci Technol.* 2021;66:102813.
21. Enayatifard R, Akbari J, Saeedi M, Morteza-Semnani K, Parvin S, Hashemi MH, et al. Investigating the effect of coated lipid nano particles of spironolactone with chitosan on their properties. *J Mazandaran Univ Med Sci.* 2018;28(162):25-36.
22. Rahimzadeh G, Saeedi M, Moosazadeh M, Hashemi SMH, Babaei A, Rezai MS, et al. Encapsulation of bacteriophage cocktail into chitosan for the treatment of bacterial diarrhea. *Sci Rep.* 2021;11(1):1-10.
23. Morteza-Semnani K, Saeedi M, Akbari J, Eghbali M, Babaei A, Hashemi SMH, et al. Development of a novel nanoemulgel formulation containing cumin essential oil as skin permeation enhancer. *Drug Deliv Transl Res.* 2022;12(6):1455-1465.
24. Abootorabi S, Akbari J, Saeedi M, Seyedabadi M, Ranaee M, Asare-Addo K, et al. Atorvastatin entrapped niosome (atrosome): green preparation approach for wound healing. *AAPS Pharm Sci Tech.* 2022;23(3):81.
25. Morteza-Semnani K, Saeedi M, Akbari J, Moazeni M, Seraj H, Daftarifard E, et al. Fluconazole nanosuspension enhances in vitro antifungal activity against resistant strains of *Candida albicans*. *Pharm Sci.* 2021.
26. Saeedi M, Akbari J, Semnani K, Hashemi SMH, Ghasemi S, Tahmasbi N, et al. Controlling atorvastatin release from liquisolid systems. *J Dispers Sci Technol.* 2022;43(3):375-384.
27. Hashemi SMH, Enayatifard R, Akbari J, Saeedi M, Seyedabadi M, Morteza-Semnani K, et al. Venlafaxine HCl Encapsulated in Niosome: Green and Eco-friendly Formulation for the Management of Pain. *AAPS Pharm Sci Tech.* 2022;23(5):149.
28. Akbari J, Saeedi M, Morteza-Semnani K, Hashemi SMH, Babaei A, Eghbali M, et al. Innovative topical niosomal gel formulation containing diclofenac sodium (niufenac). *J Drug Res.* 2022;30(1):108-117.
29. Wayne P. Clinical and Laboratory Standards Institute (CLSI): Reference method for broth dilution antifungal susceptibility testing of filamentous fungi. Carol Stream, IL: Allured Publ. Corp. 2008.
30. Shah R, Eldridge D, Palombo E, Harding I. Optimisation and stability assessment of solid lipid nanoparticles using particle size and zeta potential. *J Phys Sci.* 2014;25(1).
31. Çelik H, Karahan H, Kelicen-Uğur P. Effect of atorvastatin on A $\beta$ 1–42-induced alteration of SESN2, SIRT1, LC3II and TPP1 protein expressions in neuronal cell cultures. *J Pharm Pharmacol.* 2020;72(3):424-436.
32. Macreadie IG, Johnson G, Schlosser T, Macreadie PI. Growth inhibition of *Candida* species and *Aspergillus fumigatus* by statins. *FEMS Microbiol Lett.* 2006;262(1):9-13.
33. Radmard A, Saeedi M, Morteza-Semnani K, Hashemi SMH, Nokhodchi A. An eco-friendly and green formulation in lipid nanotechnology for delivery of a hydrophilic agent to the skin in the treatment and management of hyperpigmentation complaints: Arbutin niosome (Arbusome). *Colloids Surf B Biointerfaces.* 2021;201:111616.
34. Attwood D, Florence AT. "Physical Pharmacy: Fast Track." Pharm. Press (2008).
35. Shahraeini SS, Akbari J, Saeedi M, Morteza-Semnani K, Abootorabi S, Dehghanpoor M, et al. Atorvastatin solid lipid nanoparticles as a promising approach for dermal delivery and an anti-inflammatory agent. *AAPS Pharm Sci Tech.* 2020;21:1-10.
36. Rostamkalaei SS, Akbari J, Saeedi M, Morteza-Semnani K, Nokhodchi A. Topical gel of Metformin solid lipid nanoparticles: A hopeful promise as a dermal delivery system. *Colloids Surf B Biointerfaces.* 2019;175:150-157.
37. Avadi MR, Sadeghi AMM, Mohammadpour N, Abedin S, Atyabi F, Dinarvand R, et al. Preparation and characterization of insulin nanoparticles using chitosan and Arabic gum with ionic gelation method. *Nanomed. Nanotechnol. Biol Med.* 2010;6(1):58-63.
38. Silva LAB, Novaes Jr AB, de Oliveira RR, Nelson-Filho P, Santamaria Jr M, Silva RAB. Antimicrobial photodynamic therapy for the treatment of teeth with apical periodontitis: a histopathological evaluation. *J Endod.* 2012;38(3):360-366.
39. Abismail B, Canselier JP, Wilhelm AM, Delmas H, Gourdon C. Emulsification by ultrasound: drop size distribution and stability. *Ultrason. Sonochem.* 1999;6(1-2):75-83.
40. Suh H, Jun HW, Dzimianski M, Lu G. Pharmacokinetic and local tissue disposition studies of naproxen following topical and systemic administration in dogs and rats. *Biopharm Drug Dispos.* 1997;18(7):623-633.
41. Wingfield J, Badcott D, Appelbe GE. Pharmacy ethics and decision making. Pharm Press London. 2007.
42. Diril M, Karasulu Y, Toskas M, Nikolakakis I. Development and permeability testing of self-emulsifying atorvastatin calcium pellets and tablets of compressed pellets. *Processes.* 2019;7(6):365.
43. Kheradmandnia S, Vasheghani FE, Nosrati M, Atyabi F. The effect of process variables on the properties of ketoprofen loaded solid lipid nanoparticles of beeswax and carnauba wax. 2010.

44. Trivino A, Gumireddy A, Chauhan H. Drug-lipid-surfactant miscibility for the development of solid lipid nanoparticles. *AAPS Pharm Sci Tech*. 2019;20(2):1-9.
45. Bhalekar M, Upadhaya P, Madgulkar A. Formulation and characterization of solid lipid nanoparticles for an anti-retroviral drug darunavir. *Appl Nanosci*. 2017;7(1):47-57.
46. Müller R, Runge S, Ravelli V, Thünemann AF, Mehnert W, Souto E. Cyclosporine-loaded solid lipid nanoparticles (SLN®): Drug–lipid physicochemical interactions and characterization of drug incorporation. *Eur J Pharm Biopharm*. 2008;68(3):535-544.
47. Nath B, Roy T. Thermal characterization and screening of formulation variables of atorvastatin calcium immediate release tablet. *JSM Nanotechnol. Nanomed*. 2017;5(1):1044-1052.
48. Kelidari H, Saeedi M, Akbari J, Morteza-Semnani K, Gill P, Valizadeh H, et al. Formulation optimization and in vitro skin penetration of spironolactone loaded solid lipid nanoparticles. *Colloids Surf B Biointerfaces*. 2015;128:473-479.
49. Yarborough A, Cooper L, Duqum I, Mendonça G, McGraw K, Stoner L. Evidence regarding the treatment of denture stomatitis. *J Prosthodont*. 2016;25(4):288-301.
50. Morsy MA, Abdel-Latif RG, Nair AB, Venugopala KN, Ahmed AF, Elsewedy HS, et al. Preparation and evaluation of atorvastatin-loaded nanoemulgel on wound-healing efficacy. *Pharm*. 2019;11(11):609.
51. Lima WG, Alves-Nascimento LA, Andrade JT, Vieira L, de Azambuja Ribeiro RIM, Thome RG, et al. Are the Statins promising antifungal agents against invasive candidiasis?. *Biomed Pharmacother*. 2019;111:270-81.
52. Nyilasi I. Effect of different statins on the antifungal activity of polyene antimycotics. *Acta Biol Szeged*. 2010;54(1):33-36.
53. Bakhtiari S, Jafari S, Taheri JB, Kashi TSJ, Namazi Z, Iman M, et al. The effects of cinnamaldehyde (Cinnamon derivatives) and nystatin on *Candida albicans* and *Candida glabrata*. *Open Access Maced. J Med Sci*. 2019;7(7):1067.
54. Brillhante RSN, Fonseca XMQC, Pereira VS, dos Santos Araújo G, de Oliveira JS, Garcia LGS, et al. In vitro inhibitory effect of statins on planktonic cells and biofilms of the *Sporothrix schenckii* species complex. *J Med Microbiol*. 2020;69(6):838-843.
55. Nagpal A, Kaur J, Sharma S, Bansal A, Sachdev P. Nanotechnology-the Era Of Molecular Dentistry. *Indian J Dent Sci*. 2011;3(5).
56. Yue X, Niu M, Zhang T, Wang C, Wang Z, Wu W, et al. In vivo evaluation of a simvastatin-loaded nanostructured lipid carrier for bone tissue regeneration. *Nanotechnol*. 2016;27(11):115708.
57. Rodrigues DF, Couto ROD, Sinisterra RD, Jensen CEDM. Novel Eudragit®-based polymeric nanoparticles for sustained release of simvastatin. *Braz J Pharm Sci*. 2020;56.
58. Lefebvre M, Alshawa K, Dupont B. Antifungal activity of statins. *J Mycol Med*. 2010;20(3):212-217.